MOLECULAR DYNAMICS CALCULATION OF THE VISCOSITIES OF BIAXIAL NEMATIC LIQUID CRYSTALS

Sten Sarman

Institutionen för fysikalisk kemi

Göteborgs Universitet

S-412 96 Göteborg

SWEDEN

ABSTRACT

We have evaluated the Green-Kubo relations for the viscosities of a biaxial nematic liquid crystal by performing equilibrium molecular dynamics simulations. The viscosity varies by more than two orders magnitude depending on the orientation of the directors relative to the stream lines. The molecules consist of nine fused Gay-Berne oblates whose axes of revolution are parallel to each other and perpendicular to the line joining their centres of mass. This gives a biaxial body the length to width to breadth ratio of which is 5:1:0.4. The numerical evaluation of the Green-Kubo relations for the viscosities is facilitated by the application of a Gaussian director constraint algorithm that makes it possible to fix the directors in space. This does not only generate an inertial direcor based frame but also a new equilibrium ensemble. In this ensemble the Green Kubo relations for the viscosities are simple linear combinations of time correlation function integrals whereas they are complicated rational functions in the conventional canonical ensemble.

KEY WORDS: biaxial nematic liquid crystals; director constraint algorithms; Gay-Berne potentials; Green-Kubo relations; molecular dynamics simulations; viscosities

1. INTRODUCTION

Transport phenomena in liquid crystals are much richer than in isotropic fluids. The reason for this is that the lower symmetry of the liquid crystals allows cross couplings between thermodynamic forces and fluxes that are forbidden in isotropic fluids. The diffusion coefficients and the thermal conductivities are second rank tensors with two or three independent components depending on whether the symmetry is uniaxial or biaxial. The viscosity is a fourth rank tensor with 81 independent viscosities in the general case. In an isotropic fluid there are three independent components: the shear viscosity, the volume viscosity and the vortex viscosity. In uniaxial systems there are seven viscosities and in biaxial systems there are fifteen. There are cross couplings between tensors of different rank and parity. For example, the symmetric traceless strain rate cross couples with the antisymmetric pressure. This gives rise to director alignment phenomena in shear flows.

The first evaluation of the viscosities of a liquid crystal model system was done by Baalss and Hess in 1986 [1]. They performed a shear flow simulation of a perfectly aligned nematic iquid crystal. In order to decrease the computational work they devised a mapping of the liquid crystal onto an isotropic Lennard-Jones fluid. Equilibrium fluctuation relations for the viscosities of uniaxial nematic liquid crystals were first derived by Forster using projector operator techniques [2]. The same relations were derived by Sarman and Evans by applying the SLLOD equations of motion for planar Couette flow and linear response theory [3]. These relations were evaluated numerically for the Gay-Berne fluid [4]. In a later work we devised a Gaussian constraint algorithm that made it possible to fix the director in space [5]. This makes a director based frame an inertial frame. One also generates a new equilibrium ensemble. It turns out that the Green-Kubo relations for the various viscosity coefficients are linear combinations of time correlations function integrals in this ensemble whereas they are complicated rational functions in the conventional canonical ensemble. The Green-Kubo relations for the various viscosity coefficients have recently been generalised to biaxial nematic liquid crystals [6]. In this work we use these relations to calculate some of the viscosities of a biaxial liquid crystal. The model system consists of molecules composed of nine Gay-Berne oblates [7]. Their axes of

revolution are parallel to each other and perpendicular to the line joining their centres of mass. The length to width to breadth ratio is 5:1:0.4. This system has been shown to form biaxial nematic phases at high densities.

2. THEORY

The degree of ordering in a biaxial liquid crystal is described by two second rank order parameters [8,9]

$$Q_{00}^{2} \equiv \left\langle \frac{1}{2}(3\cos^{2}\theta - 1) \right\rangle, \tag{2.1a}$$

$$Q_{22}^{2} \equiv \left\langle \frac{1}{2}(1+\cos^{2}\theta)\cos 2\varphi \cos 2\psi - \cos\theta \sin 2\varphi \sin 2\psi \right\rangle, \tag{2.1b}$$

where θ, φ and ψ are the Euler angles relative to a laboratory based coordinate system. The first parameter is the well-known uniaxial order parameter. It is zero in isotropic phases and finite in uniaxially or biaxially symmetric phases. The other parameter is the biaxial order parameter. It is zero in isotropic and uniaxial phases and it is finite in biaxial phases. The order parameters can be defined more clearly if we form symmetric traceless order tensors based on the various principal molecular axes,

$$\mathbf{Q}^{ss} \equiv \frac{3}{2}\left(\frac{1}{N}\sum_{i=1}^{N} \hat{\mathbf{s}}_i \hat{\mathbf{s}}_i - \frac{1}{3}\mathbf{1}\right), \tag{2.2}$$

where N is the number of particles, $\mathbf{1}$ is the unit second rank tensor and $\hat{\mathbf{s}}_i$ is one of the principal axes $\hat{\mathbf{u}}_i$, $\hat{\mathbf{v}}_i$ or $\hat{\mathbf{w}}_i$ of the molecule, see Fig. 1. This gives three different order tensors, $\mathbf{Q}^{uu}$, $\mathbf{Q}^{vv}$ and $\mathbf{Q}^{ww}$. Using these definitions the order parameters can be rewritten as

$$Q_{00}^{2} = \left\langle \mathbf{e}_z \cdot \mathbf{Q}^{ww} \cdot \mathbf{e}_z \right\rangle \tag{2.3a}$$

and

$$Q_{22}^{2} = \frac{1}{3}\left\langle \mathbf{e}_x \cdot \mathbf{Q}^{uu} \cdot \mathbf{e}_x + \mathbf{e}_y \cdot \mathbf{Q}^{vv} \cdot \mathbf{e}_y - \mathbf{e}_y \cdot \mathbf{Q}^{uu} \cdot \mathbf{e}_y - \mathbf{e}_x \cdot \mathbf{Q}^{vv} \cdot \mathbf{e}_x \right\rangle, \tag{2.3b}$$

where ($\mathbf{e}_x$, $\mathbf{e}_y$, $\mathbf{e}_z$) is the base of a laboratory based coordinate system. The parameter Q_{00}^{2} is the largest eigenvalue of the order tensor $\mathbf{Q}^{ww}$. In isotropic phases this parameter is zero and it

is finite in uniaxial and biaxial phases. The parameter Q_{22}^{2} is zero in isotropic and uniaxial phases and it is finite in biaxial phases.

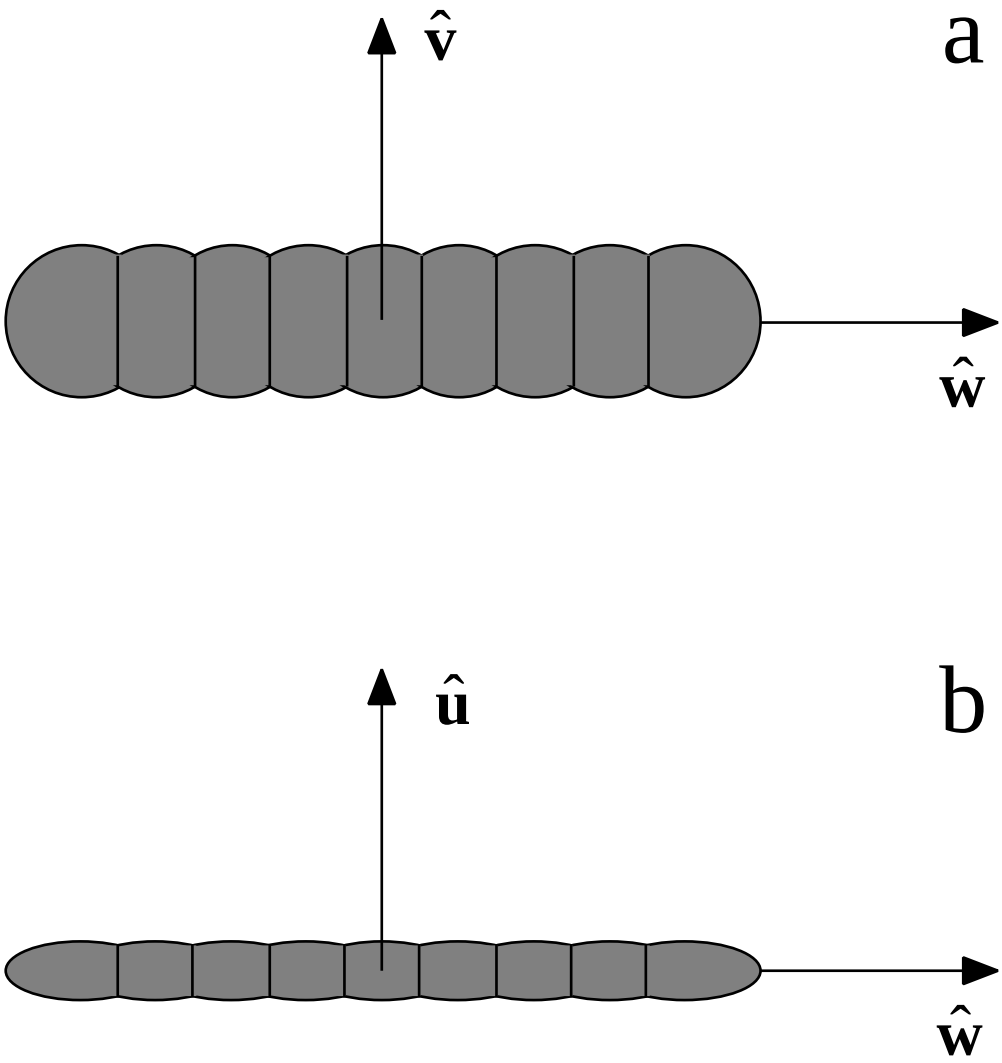

Fig. 1

Planar projections of the molecular model. a) The $\hat{\mathbf{u}}$-axis is perpendicular to the plane of the paper. b) The $\hat{\mathbf{v}}$-axis is perpendicular to the plane of the paper.

In order to make sense of these order parameters we have to define the coordinate system. One calculates the three order tensors $\mathbf{Q}^{uu}$, $\mathbf{Q}^{vv}$ and $\mathbf{Q}^{ww}$. Then one computes the largest eigenvalue of each of them. One defines the eigenvector pertaining to the largest of these eigenvalues, $\mathbf{n}_1$, as the x-direction. The eigenvector corresponding to the second largest

eigenvalue, $\mathbf{n}_2$, is defined as the y-direction. The *z*-direction is given by $\mathbf{n}_3$ which is the eigenvector corresponding the smallest eigenvalue. These eigenvectors are independent within certain limits and they are not strictly orthogonal. They are constantly diffusing on the unit sphere at angular velocities defined as $\Omega_\mu = \mathbf{n}_\mu \times \dot{\mathbf{n}}_\mu$, μ=1,2,3. This problem can be solved by applying the Gaussian director constraint algorithm, described below, to fix the directors.

We are going to use a model system consisting of rigid bodies. The equations of motion for such a system are,

$$\dot{\mathbf{q}}_i = \frac{\mathbf{p}_i}{M}, \tag{2.5a}$$

and

$$\dot{\mathbf{p}}_i = \mathbf{F}_i - \alpha \mathbf{p}_i, \tag{2.5b}$$

where

$$\alpha = \sum_{i=1}^{N} \mathbf{p}_i \cdot \mathbf{F}_i \Big/ \sum_{i=1}^{N} \mathbf{p}_i^2, \tag{2.5c}$$

$\mathbf{q}_i$ and $\mathbf{p}_i$ are the position and the linear momentum of particle *i*, *M* is the molecular mass, $\mathbf{F}_i$ is the force on particle *i* due to interactions with other particles. The parameter α is a Gaussian thermostatting multiplier that is determined in such a way that the translational kinetic energy becomes a constant of motion [10]. An important property of this thermostat is that it does not exert any torque on the system. It does consequently not interfere with the director alignment or rotation. In angular space we employ,

$$\dot{\hat{\mathbf{s}}}_i = \omega_i \times \hat{\mathbf{s}}_i \tag{2.6a}$$

and the Euler equations,

$$\mathbf{I}_p \cdot \dot{\omega}_{pi} = \omega_{pi} \times \mathbf{I}_p \cdot \omega_{pi} + \Gamma_{pi} + \sum_{\mu=1}^{3} \lambda_\mu \cdot \frac{\partial \Omega_\mu}{\partial \omega_{pi}}, \tag{2.6b}$$

where

$$\mathbf{I}_p = \begin{pmatrix} I_{puu} & 0 & 0 \\ 0 & I_{pvv} & 0 \\ 0 & 0 & I_{pww} \end{pmatrix},$$

the inertia tensor, $\hat{\mathbf{s}}_i$ equals $\hat{\mathbf{u}}_i$, $\hat{\mathbf{v}}_i$ or $\hat{\mathbf{w}}_i$, the principal axes of molecule *i*, ω_{pi} is the molecular angular velocity, Γ_{pi} is the torque due to interactions with other particles, $I_{p\alpha\alpha}$, $\{\alpha = u, v, w\}$, is

the moment of inertia around the α-axis. Do not confuse the subscript 'α' with the thermostatting multiplier α. The subscript 'p' denotes the principal frame. The Gaussian constraint multiplier λ_μ keeps Ω_μ equal to zero and thereby the director orientations are fixed in space. The $\lambda_\mu's$ are determined by the requirement that

$$\dot{\Omega}_\mu = \mathbf{0}, \qquad \mu = 1,2,3. \tag{3.2}$$

This is actually six independent equations because there are two independent components of each of the $\Omega_\mu's$ and the $\lambda_\mu's$. Provided the initial values of the $\Omega_\mu's$ are zero they will remain zero at all times and the directors will remain fixed.

The $\alpha\beta$ element of the pressure tensor is denoted by $p_{\alpha\beta}$. We employ the Irving-Kirkwood [14] definition of the pressure,

$$\mathbf{P}\, V = \left\langle \sum_{i=1}^{N} \left[\frac{\mathbf{p}_i \mathbf{p}_i}{m} - \mathbf{r}_i \mathbf{F}_i \right] \right\rangle = \left\langle \sum_{i=1}^{N} \frac{\mathbf{p}_i \mathbf{p}_i}{m} - \sum_{i=1}^{N} \sum_{j>i} \mathbf{r}_{ij} \mathbf{F}_{ij} \right\rangle, \tag{3.7}$$

where $\mathbf{r}_{ij} = \mathbf{r}_j - \mathbf{r}_i$ and $\mathbf{F}_{ij}$ is the force acting on particle *i* due to interactions with particle *j*.

3. MODEL SYSTEM AND TECHNICAL DETAILS

Our molecules consist of a string of Gay-Berne oblates [8] where the axes of revolution of the oblates are parallel to each other and perpendicular to the line joining their centres of mass. In order to decrease the number of interactions we replace the Lennard-Jones core by a purely repulsive $1/r^{18}$ core. The site-site interaction potential becomes,

$$U(\mathbf{r}_{1\alpha 2\beta}, \hat{\mathbf{u}}_1, \hat{\mathbf{u}}_2) = 4\varepsilon(\hat{\mathbf{r}}_{1\alpha 2\beta}, \hat{\mathbf{u}}_1, \hat{\mathbf{u}}_2) \left[\frac{\sigma_0}{r_{1\alpha 2\beta} - \sigma(\hat{\mathbf{r}}_{1\alpha 2\beta}, \hat{\mathbf{u}}_1, \hat{\mathbf{u}}_2) + \sigma_0} \right]^{18}, \tag{3.1}$$

where $\mathbf{r}_{1\alpha\ 2\beta}$ is the distance vector from the centre of mass of interaction site α of molecule 1 to the centre of mass of interaction site β of molecule 2, $\hat{\mathbf{r}}_{1\alpha 2\beta}$ is the unit vector in the direction of $\mathbf{r}_{1\alpha\ 2\beta}$,, $r_{1\alpha\ 2\beta}$ is the length of $\mathbf{r}_{1\alpha\ 2\beta}$ and $\hat{\mathbf{u}}_1$ and $\hat{\mathbf{u}}_2$ are the unit vectors parallel to the axis of revolution of the oblates of molecule 1 and 2 respectively. The parameter σ_0 is the length of the major axis of the oblate. The strength and range parameters $\varepsilon(\hat{\mathbf{r}}_{1\alpha 2\beta}, \hat{\mathbf{u}}_1, \hat{\mathbf{u}}_2)$ and

$\sigma(\hat{\mathbf{r}}_{1\alpha 2\beta}, \hat{\mathbf{u}}_1, \hat{\mathbf{u}}_2)$ are given by

$$\varepsilon(\hat{\mathbf{r}}_{1\alpha 2\beta}, \hat{\mathbf{u}}_1, \hat{\mathbf{u}}_2) = \varepsilon_0 \left[1 - \chi^2 (\hat{\mathbf{u}}_1 \cdot \hat{\mathbf{u}}_2)^2\right]^{-1/2}$$

$$\cdot \left\{ 1 - \frac{\chi'}{2} \left[\frac{(\hat{\mathbf{r}}_{1\alpha 2\beta} \cdot \hat{\mathbf{u}}_1 + \hat{\mathbf{r}}_{1\alpha 2\beta} \cdot \hat{\mathbf{u}}_2)^2}{1 + \chi' \hat{\mathbf{u}}_1 \cdot \hat{\mathbf{u}}_2} + \frac{(\hat{\mathbf{r}}_{1\alpha 2\beta} \cdot \hat{\mathbf{u}}_1 - \hat{\mathbf{r}}_{1\alpha 2\beta} \cdot \hat{\mathbf{u}}_2)^2}{1 - \chi' \hat{\mathbf{u}}_1 \cdot \hat{\mathbf{u}}_2} \right] \right\}^2 \tag{3.2}$$

and

$$\sigma(\hat{\mathbf{r}}_{1\alpha 2\beta}, \hat{\mathbf{u}}_1, \hat{\mathbf{u}}_2) = \sigma_0 \left\{ 1 - \frac{\chi}{2} \left[\frac{(\hat{\mathbf{r}}_{1\alpha 2\beta} \cdot \hat{\mathbf{u}}_1 + \hat{\mathbf{r}}_{1\alpha 2\beta} \cdot \hat{\mathbf{u}}_2)^2}{1 + \chi \hat{\mathbf{u}}_1 \cdot \hat{\mathbf{u}}_2} + \frac{(\hat{\mathbf{r}}_{1\alpha 2\beta} \cdot \hat{\mathbf{u}}_1 - \hat{\mathbf{r}}_{1\alpha 2\beta} \cdot \hat{\mathbf{u}}_2)^2}{1 - \chi \hat{\mathbf{u}}_1 \cdot \hat{\mathbf{u}}_2} \right] \right\}^{-1/2} . \tag{3.3}$$

The parameter $\chi \equiv (\kappa^2 - 1)/(\kappa^2 + 1)$, where κ is the ratio of the axis of revolution and the axis perpendicular to the axis of revolution and $\chi' \equiv (\kappa'^{1/2} - 1)/(\kappa'^{1/2} + 1)$, where κ' is the ratio of the potential energy minima of the side to side and the end to end configurations. The depth of the potential minimum is given by ε_0. Note that we use purely repulsive potentials, so there are no potential minima. However, we keep the values of κ', χ' and ε_0 adjusted for a Lennard-Jones potential when we replace it by a purely repulsive potential in Eq. (3.1). The molecules consist of nine interaction sites. Their axis vectors $\hat{\mathbf{u}}_i$ are parallel to each other and perpendicular to the line joining the centres of mass. The distance between the centres of mass of the oblates is $\sigma_0/2$, see Fig. 1. The parameters κ and κ' have been given the values 0.40 and 0.20 respectively. This gives a length to breadth to width ratio of 5:1:0.40. The numerical results in this work are expressed in units of σ_0, M and $\tau = \sigma_0 (M/\varepsilon_0)^{1/2}$. The moment of inertia around the $\hat{\mathbf{w}}_i$ axis is equal to $0.25 M \sigma_0^2$. The moments of inertia around the $\hat{\mathbf{u}}_i$ and the $\hat{\mathbf{v}}_i$-axes are equal to $1.8 M \sigma_0^2$. The equations of motion have been integrated by a fourth order Gear predictor corrector with a time step of 0.001τ. The cutoff radius beyond which the interaction potential and the interaction forces are set equal to zero is $1.5\sigma(\hat{\mathbf{r}}_{1\alpha 2\beta}, \hat{\mathbf{u}}_1, \hat{\mathbf{u}}_2)$. Thus the cutoff radius is orientation dependent. The expressions for the forces and the torques, which are rather complicated, are given in ref. [11]. We used cubic boundary conditions. We employed 2025 molecules which together contain 18,225 oblate Gay-Berne interaction sites.

4. CALCULATIONS, RESULTS AND DISCUSSION

We have evaluated the viscosities of this model system at a reduced density of 0.19 and a reduced temperatur of 1.00. This is very complicated and the theory is described elsewhere [12]. However, it is very easy to define and physically interpret effective viscosities

$$p_{\alpha\beta} = \eta_\gamma \frac{\partial u_\beta}{\partial r_\alpha} \tag{4.1}$$

where u_β is the velocity in the $\mathbf{n}_\beta$ direction that varies in the $\mathbf{n}_\alpha$ direction in a director based coordinate system. The $\mathbf{n}_\gamma$ direction is perpendicular to the vorticity plane, see fig. 2. Thus $\partial u_\beta / \partial x_\alpha$ is the strain rate, η_γ is the effective viscosity and $p_{\alpha\beta}$ is the $\alpha\beta$ element of the pressure tensor. This gives six different viscosities. Each of the three directors can be perpendicular to the vorticity plane and either of the two remaining directors can be perpendicular to the stream lines. If $\{\alpha,\beta,\gamma\}$ is an even permutation of {1,2,3} the viscosity is denoted η_γ and it is denoted $\eta_{-\gamma}$ for odd permutations. They can be expressed in terms of time correlation functions of the various elements of the pressure tensor,

$$\eta_1 = \eta_{2323;\Omega} + \gamma_{11;\Omega} + 2\eta_{231;\Omega} \tag{4.2a}$$

$$\eta_{-1} = \eta_{2323;\Omega} + \gamma_{11;\Omega} - 2\eta_{231;\Omega} \tag{4.2b}$$

$$\eta_2 = \eta_{3131;\Omega} + \gamma_{22;\Omega} + 2\eta_{312;\Omega} \tag{4.2c}$$

$$\eta_{-2} = \eta_{3131;\Omega} + \gamma_{22;\Omega} - 2\eta_{312;\Omega} \tag{4.2d}$$

$$\eta_3 = \eta_{1212;\Omega} + \gamma_{33;\Omega} + 2\eta_{123;\Omega} \tag{4.2e}$$

and

$$\eta_{-3} = \eta_{1212;\Omega} + \gamma_{33;\Omega} - 2\eta_{123;\Omega} \tag{4.2f}$$

We use a shorthand notation for the time correlation functions,

$$\eta_{\alpha\beta\gamma\delta;\Omega} \equiv \beta V \int_0^\infty ds \left\langle \mathring{p}^s_{\alpha\beta}(s)\, \mathring{p}^s_{\gamma\delta}(0) \right\rangle_{eq;\Omega} \tag{4.3a}$$

$$\gamma_{\alpha\beta\gamma;\Omega} \equiv \beta V \int_0^\infty ds \left\langle p^a_\alpha(s)\, \mathring{p}^s_{\beta\gamma}(0) \right\rangle_{eq;\Omega} \tag{4.3b}$$

$$\eta_{\alpha\beta\gamma;\Omega} \equiv \beta V \int_0^\infty ds \left\langle \mathring{p}^s_{\alpha\beta}(s)\, p^a_\gamma(0) \right\rangle_{eq;\Omega} \tag{4.3c}$$

and

$$\gamma_{\alpha\alpha\,;\Omega} \equiv \beta V \int_0^\infty ds \left\langle p_\alpha^a(s)\, p_\alpha^a(0) \right\rangle_{eq;\Omega} \tag{4.4c}$$

where

$$\overset{\circ s}{p}_{\alpha\beta} = \frac{1}{2}\left(p_{\alpha\beta} + p_{\beta\alpha}\right) - \frac{1}{3} Tr(\mathbf{P})$$

the symmetric traceless pressure and

$$p_\alpha^a = -\frac{1}{2}\varepsilon_{\alpha\beta\gamma}\, p_{\gamma\beta}$$

the antisymmetric pressure. The subscript *eq* denotes an equilibrium ensemble. The subscript $eq;\Omega$ denotes an equilibrium ensemble where Ω is forced to be zero. If $\alpha = \beta$ and $\gamma = \delta$ the correlation functions $\eta_{\alpha\beta\gamma\delta}$ are independent of whether Ω is constrained or not, i. e. the normal stress difference correlation functions are ensemble independent. The TCFI's involving the antisymmetric pressure are zero if Ω is unconstrained. Note that $\eta_{\alpha\beta\gamma;\Omega} = \gamma_{\gamma\alpha\beta;\Omega}$ because the pressure tensor is invariant under time reversal.

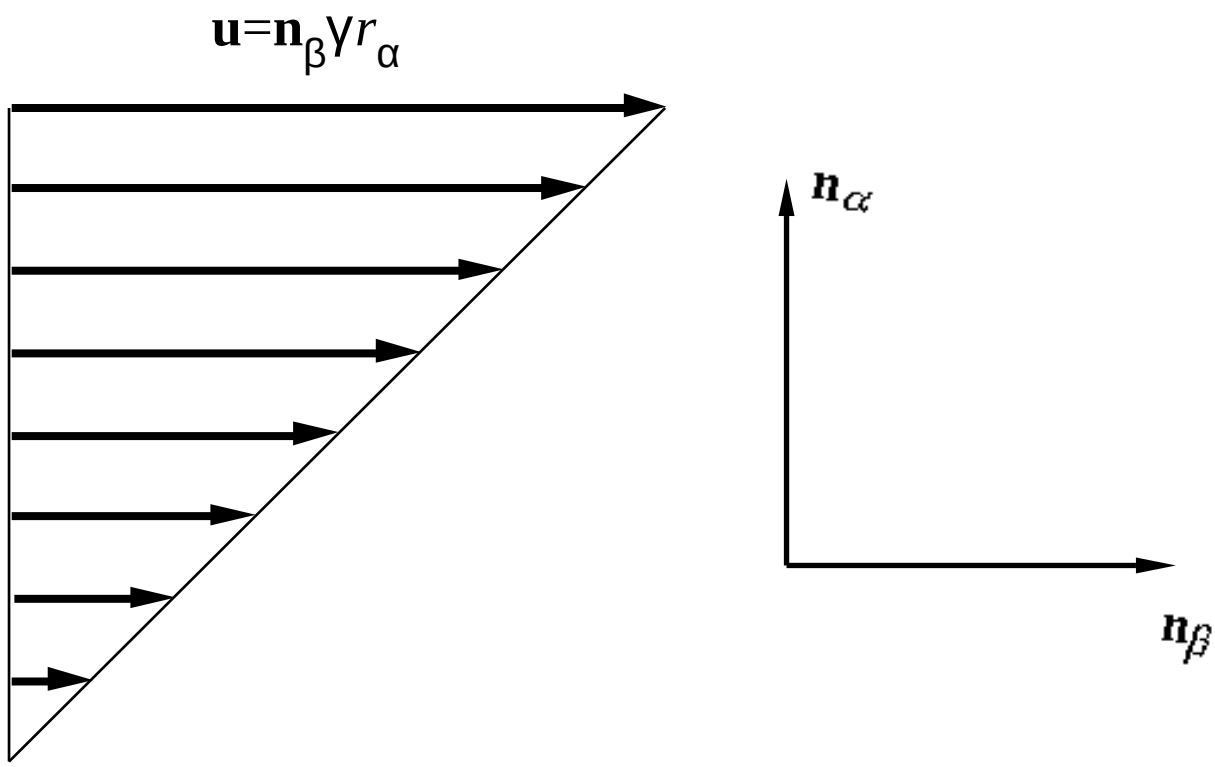

Fig. 2

A strain rate $\mathbf{u} = \gamma \mathbf{n}_\alpha \mathbf{n}_\beta$ is applied. The director $\mathbf{n}_\beta$ is parallel to the stream lines. The velocity varies in the $\mathbf{n}_\alpha$ direction. The director $\mathbf{n}_\gamma$ is perpendicular to the vorticity plane and

the plane of the paper. The axis parallel to this director has been omitted. We denote the effective viscosity η_γ if $\alpha\beta\gamma$ is an even permutation of {1,2,3} and $\eta_{-\gamma}$ for odd permutations.

The various viscosities are given in table I. We have $\eta_{-2} > \eta_1 > \eta_3 >> \eta_{-3} \approx \eta_{-1}. > \eta_2$.

Table I. The Miesowicz viscosities at a reduced density of 0.19 and a reduced temperature of 1.00.

viscosity	estimate
η_1	9.7±0.3
η_{-1}	0.57±0.06
η_2	0.19±0.005
η_{-2}	25±3
η_3	4.9±0.3
η_{-3}	0.59±0.01

The ratio of the smallest and the largest viscosity coefficients is more than two orders of magnitude. The effective viscosity is consequently very orientation dependent. It is easy to realise that η_{-2} is the largest viscosity because this is the effective viscosity when $\mathbf{n}_1$ and thereby the $\hat{\mathbf{u}}_i$ axes are parallel to the stream lines and $\mathbf{n}_3$ and the $\hat{\mathbf{w}}_i$ axes are parallel to the vorticity plane and perpendicular to the stream lines, see fig. 3. This means that it is very hard for the molecules to pass each other because the broadsides of the molecules face the stream lines and hit each other. It is also easy to realise that η_2 is the smallest viscosity because in this orientation $\mathbf{n}_3$ and the $\hat{\mathbf{w}}_i$ axes are parallel to the stream lines and $\mathbf{n}_1$ and $\hat{\mathbf{u}}_i$ are perpendicular to the stream lines and parallel to the vorticity plane. This makes it very easy for the molecules to slide past each other thus decreasing the viscosity.

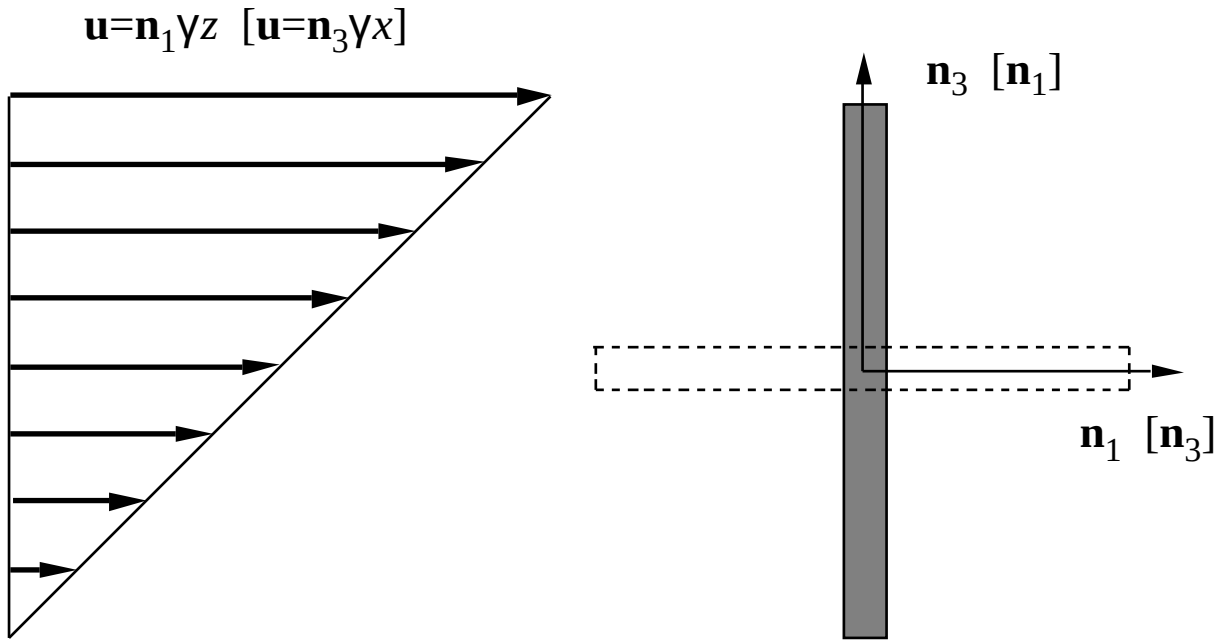

Fig. 3

Approximate orientation of the molecules when $\mathbf{n}_2$ is perpendicular to the vorticity plane. The symbols within square brackets pertain to the situation when $\mathbf{n}_3$ is parallel to the stream lines. The effective viscosity is η_{-2}. The symbols outside the square brackets pertains to the case when $\mathbf{n}_1$ is parallel to the stream lines. The effective viscosity is η_{2}.

5. CONCLUSION

We have devised a liquid crystal model potential consisting of nine oblate Gay-Berne interaction sites. Their axes of revolution are parallel to each other and perpendicular to the line joining the centres of mass. The length to breadth to width ratio is 5:1:0.4. We have removed the attractive part of the core of the Lennard-Jones core of the Gay-Berne potential and replaced it by a purely repulsive $1/r^{18}$ potential in order to reduce the number of interactions. This makes the system faster to simulate. This is useful when one wants calculate transport properties which often require very long simulation runs to converge.

In order to generate an inertial director based frame we use a director constraint algorithm that keeps the directors fixed and orthogonal. This constraint algorithm also generates a new equlibrium ensemble. Most time correlation functions and thermodynamic properties are the

same in this ensemble as in the conventional canonical ensemble. An important exception is the Green-Kubo relations for the viscosities. They are linear combinations of time correlation function integrals in the fixed director ensemble whereas they are complicated rational functions in the conventional canonical ensemble.

At high densities our liquid crystal model system forms a biaxial nematic phase. We have used the director constraint algorithm to evaluate the Miesowicz viscosities of this phase. They can be regarded as the effective viscosities when one director is parallel to the stream lines, one director is perpendicular to the vorticity plane and the last one is perpendicular to the shear plane. There are six such viscosities. They were found to be highly orientation dependent. The largest and the smallest viscosities differed by more than two orders of magnitude!

ACKNOWLEDGEMENTS

The author gratefully acknowledges support of this research by the Swedish Natural Science Council (NFR) and the National Science Foundation through grant CTS-9101326. The computations in this work were performed on the Kendall Square parallel processor of the Oak Ridge National Laboratory in Oak Ridge, Tennessee.

REFERENCES

[1] D. Baalss and S. Hess, Phys. Rev. Lett. **57**, 86 (1986);
D. Baalss and S. Hess, Z. Naturforsch. Teil A **43**, 662 (1988)

[2] D. Forster, Ann. Phys. **85**, 505 (1974)

[3] S. Sarman and D. J. Evans, J. Chem. Phys. **99**, 9021 (1993)

[4] J. G. Gay and B. J. Berne, J. Chem. Phys, **74**, 3316 (1981)

[5] S. Sarman, J. Chem. Phys. **103**, 393 (1995)

[6] S. Sarman, J. Chem. Phys. **105**, 4211 (1996)

[7] S. Sarman, J. Chem. Phys. **104**, 342 (1996)

[8] M. P. Allen, Liq. Cryst. **8**, 499 (1990)

[9] B. M. Mulder, Liq. Cryst. **1**, 539 (1986)

[10] D. J. Evans and G. P. Morriss, *Statistical Mechanics of Nonequilibrium Liquids*. (Academic Press, London, 1990)

[11] S. Sarman and D. J. Evans, J. Chem. Phys. **99**, 620 (1993)

[12] S. Sarman (submitted to J. Chem. Phys.)

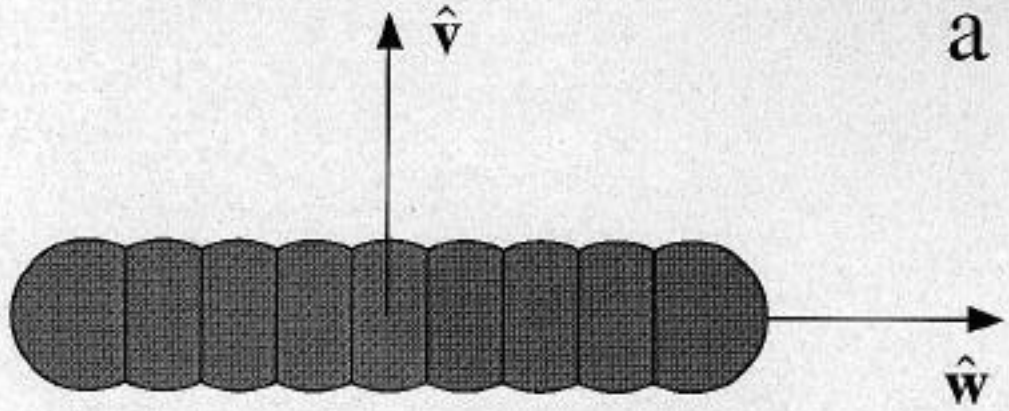

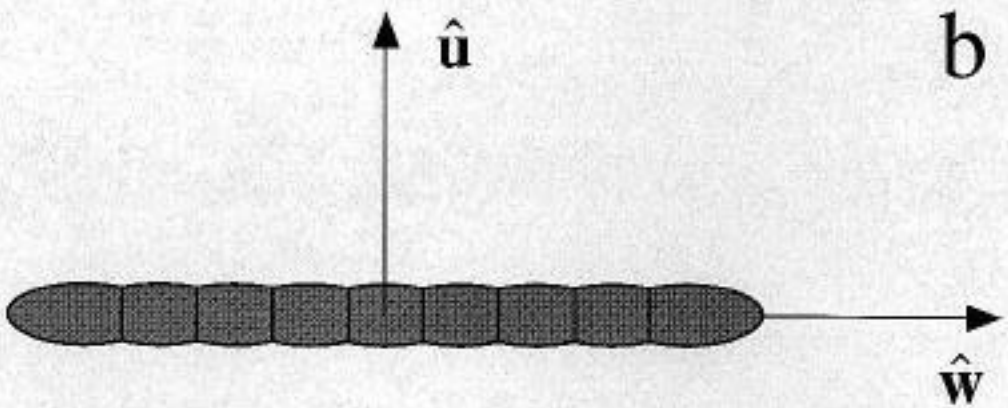

Fig. 1

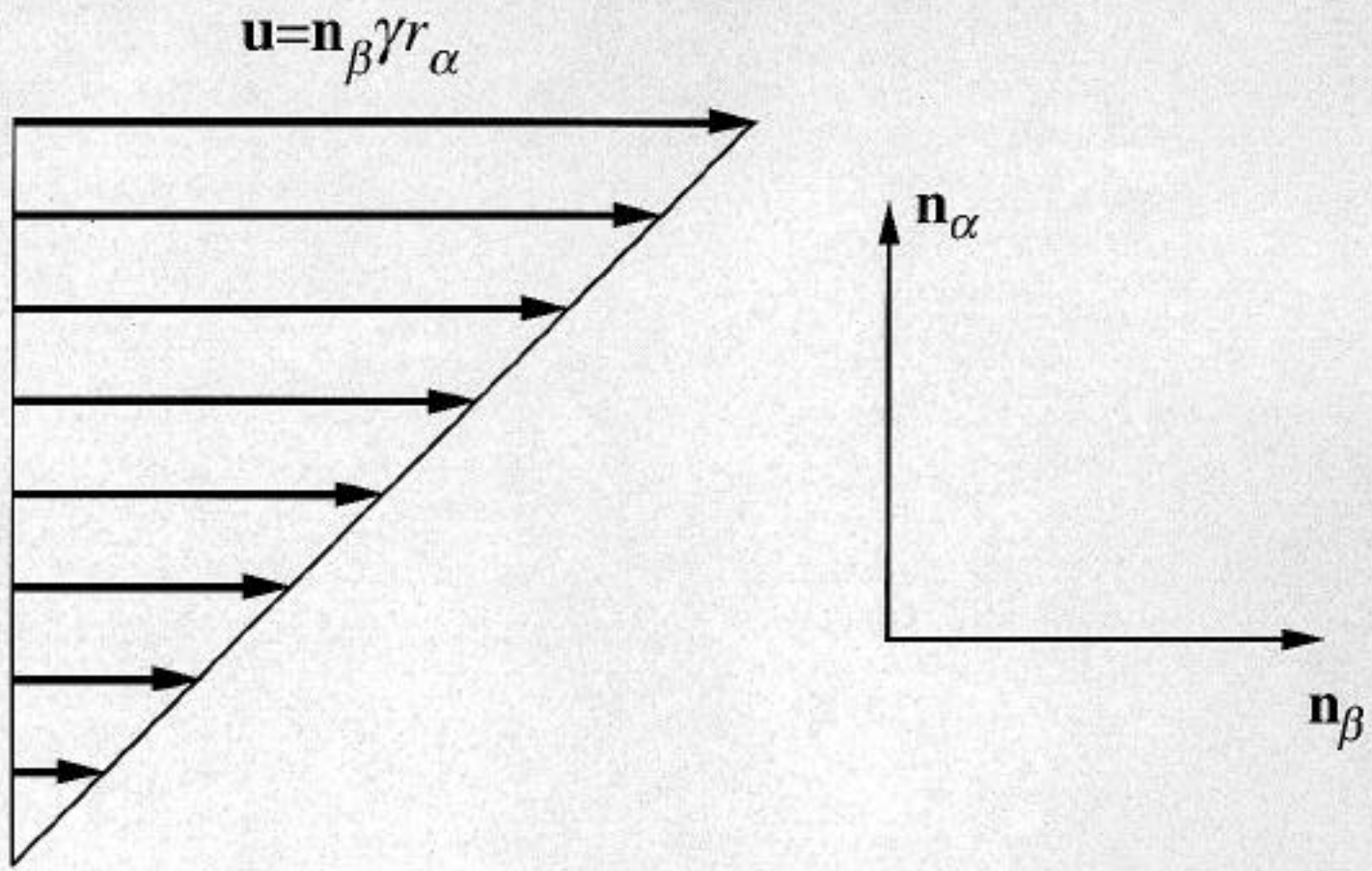
$\mathbf{u}=\mathbf{n}_\beta \gamma r_\alpha$
$\mathbf{n}_\alpha$
$\mathbf{n}_\beta$

Fig. 2

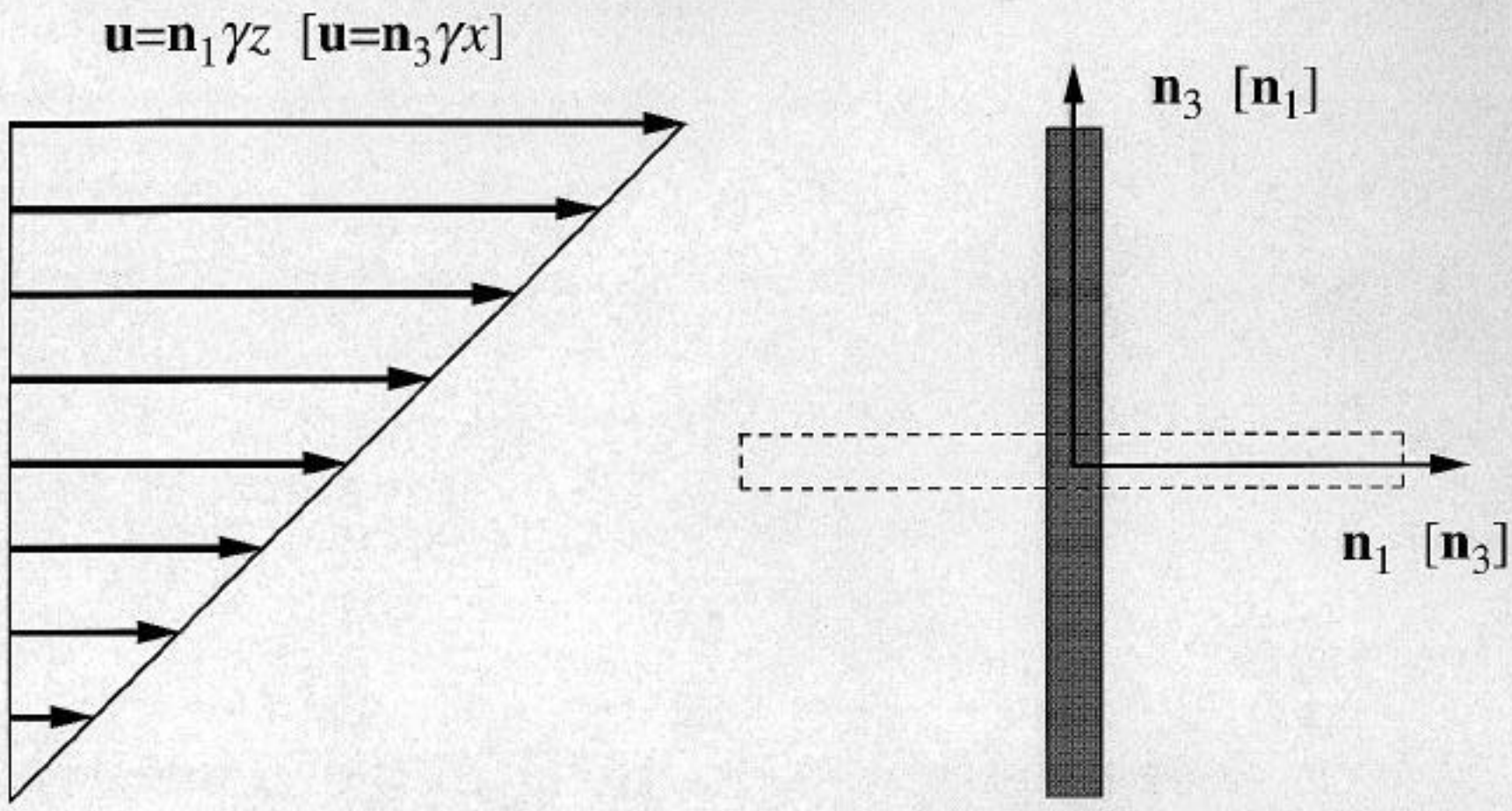
$\mathbf{u}=\mathbf{n}_1\gamma z$ $[\mathbf{u}=\mathbf{n}_3\gamma x]$
$\mathbf{n}_3$ $[\mathbf{n}_1]$
$\mathbf{n}_1$ $[\mathbf{n}_3]$

Fig. 3